

# AN IMPROVED SHOCK MODEL FOR COVERED EXPLOSIVES TAKING INTO ACCOUNT PROJECTILE AND BARRIER MATERIAL VARIATIONS

GERT SCHOLTES

TNO DEFENCE, SAFETY AND SECURITY, DEPT. ENERGETIC MATERIALS  
P.O. BOX 480, NL-2496 ZA, THE HAGUE, THE NETHERLANDS

Gert.scholtes@tno.nl

## ABSTRACT

For fragment impact and sympathetic reaction calculations, a variety of empirical and simple 1D-shock models have been developed. Some of these, like the Walker-Wasley or the Cook-Haskins-James model, use a simple critical energy criterion. The empirical Jacobs-Roslund model has a large database and is well-known in the explosive community for performing quick calculations.

For ship vulnerability and survivability calculations, TNO developed a toolbox to estimate the probability of a violent event on a ship (or other platform), based on the scenario that a munition storage is hit by e.g. a bullet or fragments from a missile attack. To obtain the proper statistical output, several millions of calculations are required. Because of this, hydrocode calculations cannot be used for this type of application, but a fast and good engineering solution is needed.

To obtain a better estimate of the occurrence of Shock-to-Detonation Transition (SDT) for covered explosives and munitions, TNO has developed an improved model which is a combination of the shock wave model at high pressure through a barrier, as described by Cook, Haskins and James, in combination with the expanding shock wave model of Green. With this model, projectile and barrier material variations can be taken into account only using a critical energy fluence parameter  $E_c$ , the shock Hugoniot of the involved materials and some other material parameters such as the density. With this model, various projectile materials, such as aluminium, tungsten or steel, or liner materials such as polyurethane layers on warheads and also internal layers such as asphalt, can be taken into account in the calculations.

This combined model gives a better fit with the experimental values for munitions response calculations, using the same critical energy fluence values for covered as well as for bare explosives. A comparison with some other models is given as well as a good, simple option for sympathetic reaction mitigation.

In this paper the theory that is implemented in the model is explained and results of the calculations for covered explosives and stored munitions will be presented and compared with other models and with experimental results.

## Introduction

Over the past years, a methodology has been developed to couple the TNO ship vulnerability code "RESIST", to a munition threat and response toolbox. Also, a statistical tool (automated spreadsheet) has been developed to estimate the probability of a prompt detonation due the impact of a certain fragment with a certain size and velocity, independent of the orientation of this fragment. The model was based on the well-known Cook, Haskins & James (CHJ) [1] shock initiation theory of a fragment impacting on an explosive with a casing in front of it. First calculations were performed for a 127 mm shell stored at e.g. the air defence and command

(LCF) frigate. The calculation was based on the CHJ [1] SDT initiation theory and parameters that were used were deduced by comparison with the Green theory [5], [7] rather than from experimental values of composition B (Comp B), the main charge explosive in the old 127 mm rounds.

Many papers were scanned in order to obtain experimental values for shock initiation of composition B/Comp B-3 (RDX-TNT composition) behind a barrier/casing and bare explosive. Also the MSIAC database FRAID was inspected [8] which revealed some data of Comp B. This showed that for bare Comp B the data points could be matched with the theory of CHJ, however it needed a different value for  $E_c$  for covered Comp B, and it did not fit the whole range. Also James, Haskins and Cook published several improvements of their shock theory showing that some changes were needed [3].

Because a good match with the experimental values could not be found, an improvement of the model was necessary. In the next paragraphs the improved model will be explained and the results of the calculation and comparison with the experimental values, found in literature and other models like Cook, Haskins and James[1] and Jacobs and Roslund (JR) [2], will be presented.

### Prompt shock initiation theory

James, Haskins and Cook [1] and Walker and Wasley [4] described a way that a shock wave of an impacting (flat) cylinder travels through a barrier and is influenced by the rarefaction wave starting at the outer edge of the cylinder traveling inwards into the shock wave (see Figure 1). The drawing shows the cross-section of an impacting cylinder with a diameter  $D_i$ , on a barrier of thickness  $d_c$  and an explosive behind this barrier.

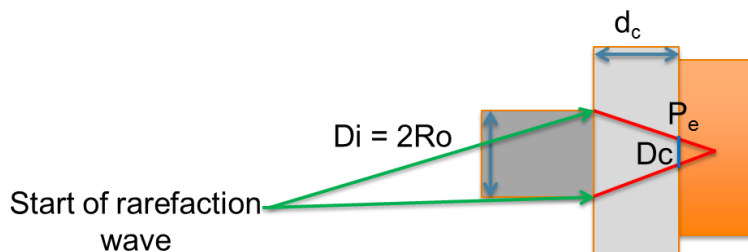


Figure 1 Shock wave at maximum pressure from a impacting fragment on an a barrier and explosive going through the different layers.

The shock wave from an impacting fragment will travel through the casing and reaches the explosive. Once entering the barrier, the pressure wave will expand in all directions but also the rarefaction will start. The 2-dimensional area (in this cross-section) having a maximum pressure in the barrier is delimited by the red lines in the drawing and giving a cone shape (3-dimensional in real life) of the shock wave at maximum pressure. As mentioned before, due to the so-called rarefaction wave, starting from the edge of the fragment, the area of maximum pressure going into the explosive is reduced to a small circle (3-dimensional, blue in Figure 1). The shock impedance calculation from the impacting projectile to the barrier and from the barrier in to the explosive can be performed, and the shock wave pressure  $P_e$ , can be determined when the impacting velocity of the projectile and the so-called shock Hugoniots of the three different materials (material parameters) are known. This has also been described in reference [7].

The CHJ theory gives an equation for the size of the area (circle indicated by the blue line in Figure 1) depending on the size of the impactor ( $D_i = 2R_0$ ) and the thickness of the barrier  $d_c$  and is:

$$R_c = R_0 - dc/U_s \sqrt{c^2 - (U_s - u_p)^2} \quad (1)$$

With  $U_s$  the shock velocity in the barrier, as a result of the impact of the projectile and  $u_p$  the particle velocity in the barrier;  $c$  is sound speed in the barrier at high pressure. To solve this problem, material properties are needed such as the Equation-of-State (EOS) giving a relation between the e.g. the shock velocity  $U_s$  in a material and the particle velocity  $u_p$ . For most materials this is can be approximated by a linear relation and has the following form:

$$U_s = C_0 + S u_p, \quad (2)$$

$C_0$  is the sound velocity in the specific material. Following Walker and Washley [4] the energy flux  $E$  going into the explosive is given by the following equation:

$$E = P_e u_p t \quad (3)$$

For a flat cylinder impacting an explosive the shock duration is  $t = D/6C_0$ , with  $C_0$  the sound velocity in the explosive. In the case of a barrier,  $D = D_c = 2R_c$ , which leads to:

$$E = P_e u_p D/6C_0 \quad (4)$$

For a certain critical amount of energy fluence  $E_c$ , the explosive will just detonate and this amount is determined by the equation:

$$E_c = P_e u_p \frac{D}{6C_0} \quad (5)$$

In this simple form, only the energy flux at the area at maximum pressure  $P_e$ , is taken into account. However, for high velocity impactors, also the pressure just near the area of maximum pressure  $P_e$ , is relatively high with respect to the minimum initiation pressure of an explosive. An impactor at a velocity of 1.5 km/s will cause the pressure in a steel barrier to rise over 30 GPa, which is much higher in comparison to an initiation pressure of an explosive of around 2 GPa (at long shock duration). So, a large decrease in pressure still leads to a relatively high pressure.

As described in reference [7], Green also showed that the impact of a projectile with a smaller diameter than the critical diameter of the explosive is still capable to initiate the explosive when the impactor velocity is high (1.5 - 3 km/s, see Figure 2).zl

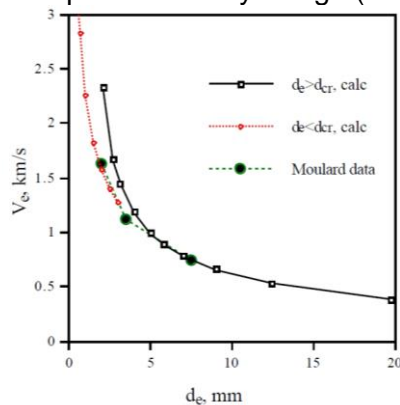


Figure 2 Shock initiation of explosives showing the minimum projectile velocity as a function of the diameter  $d_e$ ; even when the impactors is smaller than the critical diameter of the explosive, a high impacting small fragment is still capable to initiate the explosive due to a high velocity.

From these experimental results it is clear that the CHJ model is not capable to explain the detonation of explosives behind thick barriers. Roughly their theory tells that when a barrier is about half the impacting diameter  $D_i$ , a prompt detonation of the explosive is not possible anymore. However, these experiments show that at very high impactor velocities, an explosive can still be initiated.

Figure 3 explains the theory of Green. The impactor with diameter  $d_e$ , is smaller than the critical diameter  $d_{cr}$  of the explosive. However, the high shock pressure is expanding in the explosive (or the barrier first) and will grow to such a size, larger than the critical diameter  $d_{cr}$ , while the decreased pressure (due to the expansion) still has a value capable to initiate the explosive.

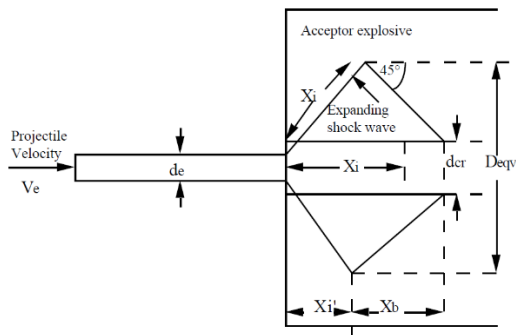


Figure 3 Shock wave of a small impactor on an explosive explained by Green.

The detailed description of the theory can be found in reference [7]. The new, improved shock model described in this paper is based on this idea combined with the CHJ energy fluence. Figure 4, shows the effect of the two combined ideas. The part of the high shock wave from the impactor is the same as CHJ and the energy fluence has the value:

$$E_{H\&C} = P_h u_p \frac{D}{6C_0} \quad (5a)$$

With  $P_h$  the maximum (high) pressure in the explosive. For the expanding shock wave in the barrier (Figure 4),  $P_{eqv}$  has to be determined.

The impactor with diameter  $D_i$  and velocity  $V$  hits a barrier of thickness  $d_c$ . The expanded wave travels through the barrier and grows to a size  $D_{eqv}$ , at a lower pressure  $P_{eqv}$ .

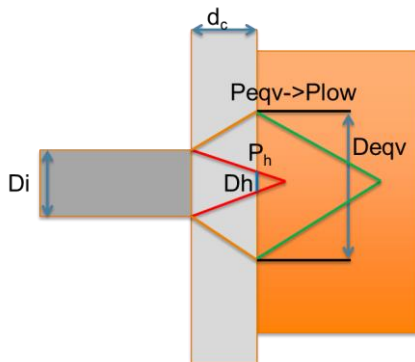


Figure 4. Shock wave from impactor on barrier and explosive, combining a high pressure decreasing shock energy and an expanding low pressure shock wave.

From reference [7] we have:

$$D_{eqv} = D_i + \sqrt{2}X_i \text{ with } X_i' = X_i/\sqrt{2} \quad (6)$$

$$P_{eqv} D_{eqv} = P_b D_i \text{ and so } P_{eqv} = P_b D_i/D_{eqv} \quad (7)$$

with  $X_i$  is the radius of curvature of the expanding shock front (see Figure 3). The shock wave pressure into the explosive is assumed to decrease uniformly with distance from the explosive surface to a depth ,  $X_i' = X_i/\sqrt{2}$ ,  $P_b$  = the initial pressure in the barrier after impact. Combining eqs. (6) and (7) gives the equation for  $P_{eqv}$ :

$$P_{eqv} = P_b / (1 + \frac{\sqrt{2} X_i}{D_i}) \quad (8)$$

From  $P_{eqv}$  (in the barrier),  $P_{low}$  in the explosive can be solved by the shock impedance matching equations as described in reference [7] as well as the  $P_h$  was determined by the impedance matching with  $P_b$ . This leads to a set of equations for the different boundaries:

$$P - P_0 = \rho_0 u_p U_s (P_0 \ll P) \quad (9)$$

and the shock Hugoniot of materials  $U_s = C_o + S u_p$

$$P_1 = P_2 = \rho_1 U_{s1} (v_{projectile} - u_p) = \rho_2 U_{s2} u_p \quad (10)$$

and  $u_{p1} = u_{p2} = u_p$

Analyses lead to a quadratic equation for the particle velocity  $u_p$  which can be solved with the standard solution for quadratic equations. Once  $u_p$  is known,  $U_s$  and  $P$  can be determined.

The expanding shock energy fluence part has the same form as the high pressure-part but with the lower pressure  $P_{low}$  and larger  $D_{eqv}$  diameter. The total form of the energy fluence will now have the form:

$$E_{total} = \{ E_{expanding} \pi [ (D_{eqv}/2)^2 - R_c^2 ] + E_{H\&C} \pi R_c^2 \} / \{ \pi (D_{eqv}/2)^2 \} \quad (11)$$

With

$$E_{H\&C} = P_h u_{p,high} R_c / (3 C_{e,high}) \text{ and } E_{expanding} = P_{low} u_{p,low} D_{eqv} / (6 F C_{e,low}) \quad (12a, 12b)$$

With  $P_h$  the high pressure,  $P_{low}$  the low pressure of the shock wave, both in the explosive (calculated by impedance matching). From  $P_{low}$  the value  $u_{p,low}$  can be determined;  $u_p$  is determined by the same impedance matching calculation as for  $P_h$ . Also the sound velocities  $C_{e,high}$  at high and  $C_{e,low}$  at low pressure have to be determined for both pressure levels in the explosive according to:

$$C_e = (u_{se} - u_{pe})(u_{se} + S_e u_{pe}) / u_{se} \quad (13)$$

$F$  is a shape factor of the curved shock front going in to the explosives. Following the theory, a certain minimal amount of energy fluence  $E_c$  is needed to (shock) initiate a certain explosive material. Once the value of  $E_c$  is known, the minimum projectile velocity can be determined that transfers this amount of energy into the explosive. So:

$$E_c = E_{total} \quad (14)$$

The model can be solved in e.g. an Excel spreadsheet to obtain a solution for the minimal velocity to initiate a certain explosive.

## Sympathetic reaction geometries

The theory for a sympathetic reaction as described by Victor [7], is used for the sympathetic reaction calculations. For sympathetic reactions three scenarios are of importance. The first scenario is when a donor and acceptor munition are at a rather large distance (distance > two times the radius of the donor munition). The effect of the donor charge is only a fragment of a certain size and maximum fragment velocity of the donor charge. The second scenario is what we call the one-on-one situation, and shown in Figure 5. The donor warhead (green) is expanding as a balloon and the acceptor munition on top of the donor or just next to the donor (magenta and cyan) is hit by the expanding casing of the donor. The impact is not a single fragment but a slice of the donor casing and is generally larger than a single fragment from the donor. However, the velocity is very much dependent on the distance between the donor and acceptor charge.

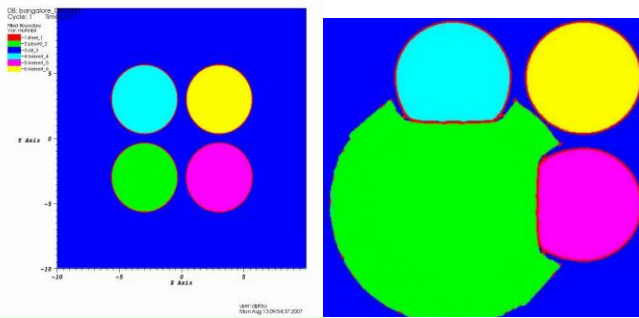


Figure 5 Sympathetic reaction scenarios with the detonating donor charge (green) impacting the two near shells (Cyan and magenta) and a large, rather flat fragment impacting the yellow donor shell (calculation performed by ARDEC).

A last scenario, also shown in Figure 5, is the effect on the charge that is diagonally located with respect to the donor charge (yellow). The expanding donor (green) is confined in between the two charges on the top and on the left (cyan and magenta, respectively). Because of this effect, a rather flat expanding casing hits the acceptor charge, leading to an effective and large impacting plate on the donor charge. This scenario is called the confined-stack scenario.

## Velocity of the expanding donor casing/fragment

A casing of a detonating warhead reaches its maximum velocity after 1.6 – 1.8 [7] times its original radius. The maximum casing or fragment velocity can be derived from the well-known Gurney equations, as described in reference [7]. After the detonation of the explosive, the velocity of the expanding casing will increase as a function of travelling distance and will reach its maximum velocity after some distance. This maximum velocity depends on the type of explosive but also on the amount of explosive in relation to the amount of casing material that has to be accelerated. A good estimate of the velocity of an expanding casing is the following:

$$\frac{V_R}{V_{Gurney}} = Max \left( \frac{V_0}{V_{Gurney}}, \left[ K \left( 1 - \left( \frac{R_D}{R_E} \right)^2 \right) \right]^{1/2} \right) \quad (14)$$

$$V_0 \sim \left\{ \left[ \left( C_{0c}^2 + 4S_c \frac{P_c}{\rho_{0c}} \right)^{1/2} - c_{0c} \right] / 2S_c \right\} \frac{(R_D - t_c)}{R_D} \quad (15)$$

$$P_c \sim \rho_{0c} P_{cj} / (\rho_{0c} + \rho_{0e}) \quad (16)$$

where

$$V_{Gurney} = \sqrt{\frac{2E}{\left(\frac{M}{C} + \frac{n}{n+2}\right)}} \quad (17)$$

with  $M$  the mass of the warhead casing,  $C$  de mass of the explosive,  $n$  a shape factor (which is 2 for a cylindrical shape, such as a warhead).  $\sqrt{(2E)}$  is the Gurney-energy (a constant for a given explosive),  $R_D$  and  $R_E$  are the radius of the original donor warhead and the expanding donor casing,  $c_{oc}$ ,  $s_c$ ,  $\rho_{oc}$ ,  $\rho_{oe}$ , the shock Hugoniot values and the density of the casing and the explosive, respectively.  $P_{cj}$  is the so-called Chapman-Jouget pressure of the explosive,  $t_c$  the wall thickness of the warhead.  $K$  is a constant which is about 1.35 for an explosive that puts the major part of the energy in the acceleration of fragments.

Victor [7] implemented these equations in an Excel spreadsheet for sympathetic reaction calculations. The method has been improved by TNO and is now implemented in the core of the TNO toolbox. For the sympathetic reaction calculation, first the effective diameters of the ono-on-one and diagonal fragment have to be determined. Victor gives an extensive explanation how to obtain an estimate for the maximum effective diameter based on the distance between the shells and the velocity of the expanding casing/fragment. For the one-on-one scenario the velocity is also determined as a function of the distance between the shells using equation (14) - (17). For the diagonal fragment the maximum velocity using the Gurney equation is taken. Using the shock model described in the previous section, the sympathetic reaction scenarios can then be obtained.

### Comparison with experiments from literature and other models

Most experimental shock studies have been performed in the past and MSIAC summarized most of these results in the FRAID database [8]. One of the test series in the database is a series of tests that has been performed with composition B by DOSG in the UK. They performed fragment impact tests with 13.15 and 20 mm flat-ended cylinders on Comp B and varied the barrier in front of the explosive. For comparison, several calculations have been performed using the current model, the old CHJ-model and that of JR using the parameters from reference [6] for Comp B.

Figure 6 shows the result of these models in comparison to the experimental data. It is clear that the CHJ model (dashed curves) does not fit the data correctly, certainly not for thick barriers. The JR model fits rather good but the current model appears to follow the data more precise for values of  $E_c$  between 1.85 and 2.1 MJ/m<sup>2</sup>.

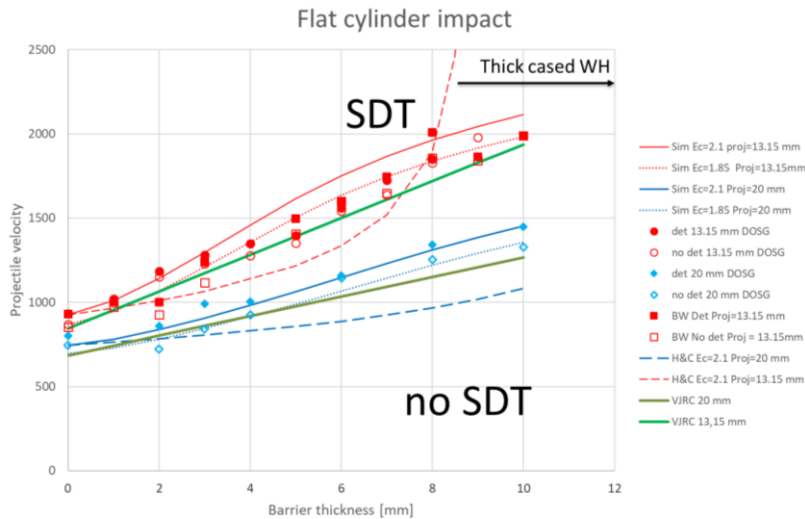


Figure 6 Comparison of the experimental values of a fragment impact test and the results from the models of HCJ (dashed curves), JR (thick, solid curves) and the model described in this paper (thin solid and dotted curves).

As mentioned in the introduction, the advantage of the JR model is that it has a large database of parameters, for all kind of in-service explosives. However, the model is not capable to simply change the impact material or the barrier material. Figure 7 shows the results of some calculations according to the JR model in comparison with the current model. These models are quite comparable for the 13.15 mm flat steel impactor with a barrier of steel and a value of  $E_c=1.85 \text{ MJ/m}^2$  for Comp B for the current model (dotted and orange line). However, in case the impactor and barrier are made from aluminum, the JR model is not capable to give a good estimate because it is based on steel. For the current model this can be easily done by replacing the shock Hugoniots of steel with those of aluminum. The results for the critical velocity of a projectile leading to a detonation of an explosive as a function of the barrier thickness are also shown in Figure 7, as well as some other material combinations.

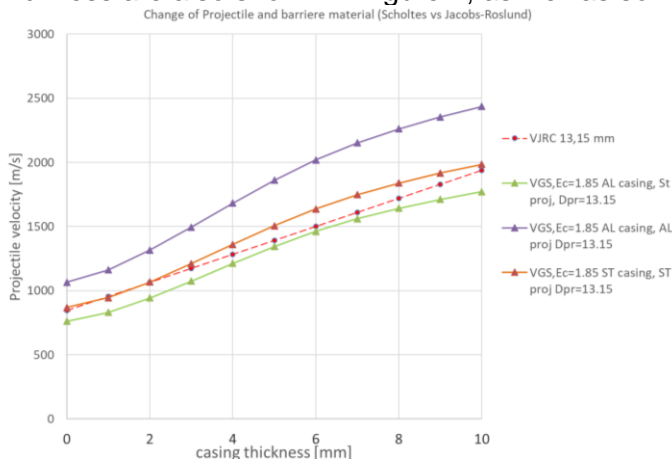


Figure 7 Comparison of the results from the JR and the current model for a steel impactor and steel barrier as well as for aluminum projectiles or barriers. The graph shows the critical projectile velocity leading to a detonation of an explosive as a function of the thickness of the casing (barrier).

Figure 8 shows the critical velocity of the impactors as a function of the projectile diameter for the three types of barriers. A warhead having a casing of 14 mm steel would not survive the impact of a 18 mm impactor at a velocity of about 1800 m/s (two points in the graph at  $x=18$  mm fragment diameter). Also the warhead having an extra layer of polyurethane (PU) inside the casing will not survive this impact. However, the warhead having a 4 mm PU layer at the outside of the casing will not detonate (for the 18 mm impactor a velocity of about 2200 m/s). Due to the thin PU layer this warhead can survive a fragment impact of an 18 mm diameter

fragment at velocities up to 2200 m/s. This is exactly the outcome of the series of experiments, showing that the warhead survives several impacts of 18 mm diameter projectiles at 1800 m/s, responding in a mild burning of the warhead.

Influence of PU layer on outside

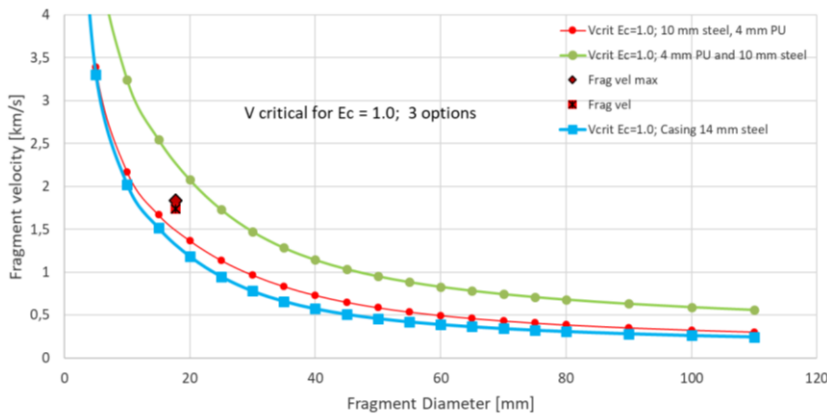


Figure 8 Calculation of the critical velocity of a steel fragment leading to a detonation of a warhead. Three different scenarios are shown: a 14 mm steel barrier, a 10mm-4mm (steel-PU) barrier and 4mm-10 mm (PU-steel) barrier. As shown in a series of experiments the calculation also confirms that a warhead with the third type of barrier can survive fragment impact threats at a velocity of about 1800 m/s or even higher.

### Estimating the value of the Critical Energy Fluence

Because the critical energy fluence parameter  $E_c$  is unknown for many explosives, it is necessary to estimate this parameter. For a rough estimate, a comparison can be made with the results from JR, as shown in Figure 7.  $E_c$  can be varied and compared with the JR results. The value of  $E_c$  that shows the best fit with the JR values is the best estimate for  $E_c$ . This can also be done by comparing the results with other methods like the Green model.

However, when better estimates are desired, the parameter can be estimated by performing a Water Gap Test (WGT) or Large Scale Gap Test (LSGT). Verbeek and Bouma [9] but also Wurster [10] performed computer studies to compare the energy fluence of a certain explosive with the results of the WGT and LSGT. In these computer studies, first the model had to be calibrated with the gap length-pressure calibration curve of the gap tests. Once the model shows good agreement, a series of calculations can be performed. Because the pressure in the gap material is influenced by the rarefaction wave from the edge of the cylinder, the pressure as a function of time also changes as a function of the radius. For the calculation of the energy fluence the surface averaged maximum pressure is calculated using the following equation:

$$\overline{P_{max}} = \frac{1}{\pi R^2} \int 2\pi r P_{max}(r) dr \quad (18)$$

with  $R$  the radius of the cylinder. An example for the WGT at a gap of 23 mm is shown in Figure 9 on the left. The surface averaged maximum pressure is lower than the maximum pressure measured at the axis in the gap tests. Doing this for all gap lengths, a comparison can be made between the detonation pressure of the gap test of the explosive of interest and the critical energy fluence determined by the following equation:

$$E_c = \int \overline{P_{max}} \cdot u_{p,x} \cdot dt \quad (19)$$

The result from reference [10] are shown on the right hand side of Figure 9 for the 21 mm WGT as well as for the 50 mm LGST. So, the obtained detonation pressure of the investigated explosive can be directly translated to the critical energy fluence of that explosive.

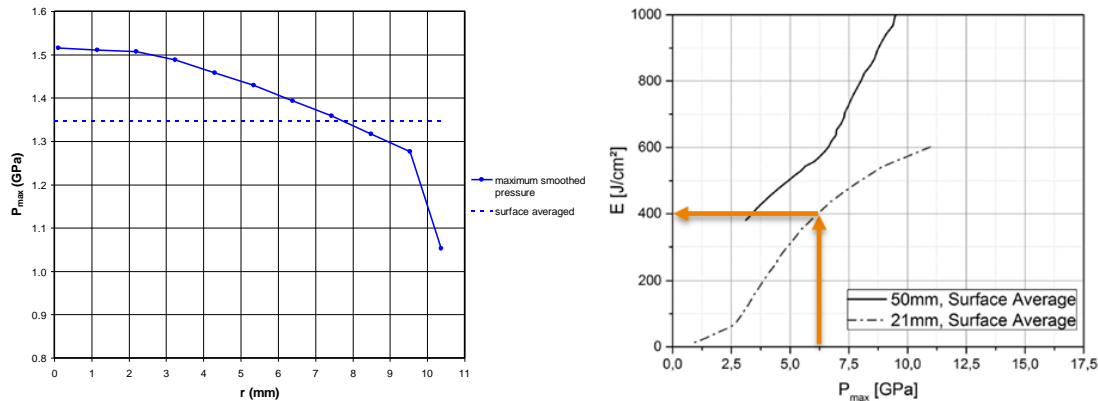


Figure 9 Left: the surface averaged maximum pressure at a gap length of 23 mm in the 21 mm WGT. Right: the relation for the Gap Test detonation pressure  $P_{max}$  and the corresponding  $E_c$  for an explosive for the 50 mm LSGT as well as the 21 mm WGT.

Also other methods are under investigation at TNO. Yadav et al. [11] derived an equation for  $E_c$  (equation 20) as a function of the shock Hugoniot parameters  $a_x$  and  $b_x$ , the detonation velocity  $D_j$ , the specific heat ratio of detonation products  $r$ , the density  $\rho_o$  and the value of the reaction zone length  $\delta$  of the explosive. Together with the value of the reaction zone length using a so-called shock-induced polarization experiment, described in e.g. ref [12], a value of  $E_c$  can be estimated.

$$E_c = \frac{\rho_o D_j \delta \left[ \frac{D_j - a_x}{2b_x} + \frac{D_j}{2(r+1)} \right]^2}{D_j - \left( \frac{D_j - a_x}{2b_x} + \frac{D_j}{2(r+1)} \right)} \quad (20)$$

## Summary

A new SDT model has been developed for quick calculations of the critical velocity of a projectile impacting a confined explosive leading to an SDT reaction. The model uses the critical energy fluence parameter  $E_c$  of an explosive and some other well-known parameters such as the shock Hugoniot and densities of the explosives and materials. The model can handle variations in the impactor materials, barrier materials as well as multiple barrier layers. Although the value of  $E_c$  is not available for all known in-service explosives, estimates can be made using other models such as Jacobs-Roslund or Green. But also the Water Gap Test or Large Scale Gap Test results can be used to convert the detonation pressure of a certain explosive into the value of  $E_c$ . Once all parameters are known, quick calculations can be performed for all kind of scenarios. The method can also be implemented in several other codes and statistical analyses can be performed to estimate the probability of a detonation when a tumbling fragment is hitting a given munition item in a munition store. The next step is the calculation of the probability of a sympathetic reaction of adjacent munition items and the probability of a mass-detonation of the complete stockpile. This method will be used by TNO to investigate the safety of the storage situations onboard ships of the Dutch Navy.

## REFERENCES

- [1] M. Cook, P. Haskins, and H. James, "Projectile impact initiation of explosive charges", *Preprints from the 9th detonation symposium*, pp 615-623, 1989

- [2] J.W. Roslund, N.L. Watt and Coleburn, "Initiation of warhead explosives by the impact of controlled fragments : normal impact", Technical Report NOLTR-73-124, Naval Ordnance Laboratory, White Oak, MD, August 1974
- [3] H. James, P. Haskins, and M. Cook, "Prompt shock initiation of cased explosives by projectile impact, Pyrotechnics, explosives, propellants, vol 21, pp 251-257, 1996
- [4] F.E. Walker and R.J. Wasley, "Critical energy for shock initiation of heterogeneous explosives", Explosive Stoffe, 17, 9, 1969
- [5] LeRoy Green, "Shock initiation of explosive by the impact of small diameter cylindrical projectiles", 7<sup>th</sup> int Detonation symposium 1981
- [6] M. Crull, M. Swisdak, and S. Hamilton; Methodologies for calculating primary fragment characteristics, Report DDESB TP 16 Revision 4, Department of Defense Explosives Safety Board, USA, April 2012
- [7] A. Victor, , "Guide to spreadsheet calculations for insensitive munitions applications", supplemental text, April, 1996
- [8] Frédéric Peugeot, "The NIMIC FRAGment Impact Database (FRAID)", MSIAC report O-090, August 2004
- [9] Ries Verbeek, Richard H. B. Bouma, "Evaluation of the energy fluence in the small scale gap test", Propellants, Explosives, Pyrotechnics, 2011, 36, 16 – 21
- [10] Sebastian Wurster, "Evaluation of the James initiation criterion in the 21 mm and 50 mm PMMA gap test", Propellants, Explosives, Pyrotechnics, 2017, 42, 749–753
- [11] H.S. Yadav, S.N. Asthana, and A. Subhananda Rao, Critical shock energy and shock and detonation parameters of an explosive, Defence Science Journal, Vol. 59, No. 4, July 2009, pp. 436-440
- [12] R. R. Jsselstein, Reaction zone measurements in high explosive detonation waves by means of shock-induced polarization", Combustion and Flame, 66 (1986) 27-35